Journal of Marine Science and Technology

Volume 21 | Issue 2 Article 9

EFFECTS OF SURFACE ROUGHNESS AND FLOW RHEOLOGY ON THE EHL OF CIRCULAR CONTACTS WITH POWER-LAW FLUID

Li-Ming Chu
Department of Mechanical and Automation Engineering, I-Shou University, Kaohsiung City, Taiwan, R.O.C, hmchu@mail.isu.edu.tw

Jaw-Ren Lin
Department of Mechanical Engineering, Taoyuan Innovation Institute of Technology, Jhongli City, Taoyuan County, Taiwan, R.O.C

Hsiang-Chen Hsu
Department of Mechanical and Automation Engineering, I-Shou University, Kaohsiung City, Taiwan, R.O.C

Yuh-Ping Chang
Department of Mechanical Engineering, Kun Shan University, Tainan, Taiwan, R.O.C.

EFFECTS OF SURFACE ROUGHNESS AND FLOW RHEOLOGY ON THE EHL OF CIRCULAR CONTACTS WITH POWER-LAW FLUID

Acknowledgements

The authors would like to express their appreciation to the National Science Council (NSC 99-2221-E-214-011) in Taiwan for financial support.

Journal of Marine Science and Technology, Vol. 21, No. 2, pp. 175-181 (2013)
DOI: 10.6119/JMST-012-0206-7

EFFECTS OF SURFACE ROUGHNESS AND FLOW RHEOLOGY ON THE EHL OF CIRCULAR CONTACTS WITH POWER-LAW FLUID

Li-Ming Chu[1], Jaw-Ren Lin[2], Hsiang-Chen Hsu[1], and Yuh-Ping Chang[3]

Key words: EHL, roughness, power law fluids, average flow model.

ABSTRACT

The coupled effects of surface roughness and flow rheology on the Elastohydrodynamic lubrication (EHL) circular contact problems are analyzed and discussed. The average flow model is adapted for the interaction of the flow rheology of lubricant and surface roughness. The averaged Reynolds type equation, the rheology equations, the elastic deformation equation, and the force balance equation are solved simultaneously. The multilevel multi-integration (MLMI) algorithm and Gauss-Seidel iteration method are utilized to calculate the film thickness and pressure distributions. The effects of flow index, Peklenik number, and standard deviation of composite surface roughness on the film thickness and pressure distributions are discussed. The results show that the transverse type roughness and standard deviation of composite roughness enhance the pressure and film thickness in the central contact region. Moreover, the greater the flow index is, the greater the pressure distribution is in the central contact region, and the greater the film thickness is in all regions.

I. INTRODUCTION

Elastohydrodynamic lubrication (EHL) describes the mode of lubrication in higher pressure and thinner lubricating film that one meets in many mechanical components such as gears, cams, rolling element bearings, and so on. In order to improve film thickness and lubricant viscosity, the polymeric fluid additives are added to the base oil. Therefore, The linear relationship between the shear stress and the rate of shear is not valid for many lubricants. So the use of non-Newtonian fluids as lubricants has become more important with the development of modern industrial materials. In addition, the surface imposed during manufacturing is not perfectly smooth. The film may then be as thin as the asperities collide. In EHL problems, the film thickness is usually comparable to the height of surface roughness. Therefore, it is important to estimate the pressure distribution and film thickness in the contact zone, for better understanding of EHL taking account of the rheology and surface roughness.

The lubricant rheology affects the lubricant film thickness and traction coefficient which are closely related to the power loss and wear of surfaces. To improve the tribology performance in the contact zone. The on-Newtonian characteristics have been invariably observed in various lubrication processes. This may be due to the high shear rate and the high pressure gradient, or due to additives. Various theories have been developed and analyzed to describe the flow behaviour of non-Newtonian lubricants. Some of which have been successfully applied in lubrication problems, such as continuum models of micropolar fluids [12, 20], continuum models of couple stress fluids [9, 24]. Both theories have been able to describe the structure of the additives and their coupling effect on the bulk flow of the lubricant. In addition, other non-Newtonian models has been presented by several researchers, such as Ree-Eyring model [2], Generalized Maxwell model [25], Bair-Winer model [1], Ivonen-Hamrock model [15], Circular fluid model [16], and Power-law models [10]. Each theory has its advantages and disadvantages to lubrication problems. However, In engineering practice, lubricants are often modeled with the power law fluid which accurately characterizes both pseudoplastic and dilatant fluids—two important classes of non-Newtonian lubricants. It is because of such wide coverage in the analysis of lubricants together with its mathematical simplicity that the power law fluid model has been preferred for application in the present problem. This power law model has found wide application in various lubrication problems [3, 8, 23].

In EHL contacts roughness and surface texture substantially affect the formation of a lubricating oil film between the contacting bodies, especially in lubricative elements working

Paper submitted 04/08/11; revised 12/24/11; accepted 02/06/12. Author for correspondence: Li-Ming Chu (e-mail: hmchu@mail.isu.edu.tw).
[1] *Department of Mechanical and Automation Engineering, I-Shou University, Kaohsiung City, Taiwan, R.O.C.*
[2] *Department of Mechanical Engineering, Taoyuan Innovation Institute of Technology, Jhongli City, Taoyuan County, Taiwan, R.O.C.*
[3] *Department of Mechanical Engineering, Kun Shan University, Tainan, Taiwan, R.O.C.*

in the boundary lubrication regime. Therefore, the effects of surface roughness become important on thin film lubrication as the standard derivation of the composite rough surfaces is comparable to the local film thickness. Two widely used tools were proposed in modeling the surface roughness: the stochastic analysis [19] and deterministic analysis are [14]. The deterministic model uses measured surface topography to calculate pressure distribution and film distribution. It takes time and requires excellent computers to trace all the asperities of the two lubricating surfaces to obtain the convergence of the solution. The statistic characteristics of real rough surface can be mathematically approximated by a stochastic process with Gaussian heights distribution. The Christensen's stochastic process theory [7] has been extended to EHL line contact and the effect of longitudinal roughness on the film thickness has been discussed [6]. The most commonly used approach is to solve Reynolds equation with the assumption of smooth surfaces and use 'flow factors' to statistically compensate for the surface roughness. An average flow model [19] taking into account the asperity contact pressure calculated from the force compliance relationship derived by Greenwood and Tripp [13] has been used by several researchers [22, 28] in order to describe the effects of the surface roughness pattern, film factor, and operating conditions on the performance of EHL. The average flow model has the advantage of being easy to apply to the distributed roughness problems. Several workers [5, 27] have incorporated effects of surface roughness in EHL analysis.

The combine effects of lubricant's rheological character and surface roughness of a hydrodynamic journal bearing were studied by Li *et al*. [17]. So far, the study of the coupling effects of power law fluids and surface roughness on the EHL circular contact problems is not valid. The present analysis investigates the coupling effects of flow rheology of the power law and surface roughness on the EHL circular contact problems numerically by solving the average Reynolds type equation, elasticity deformation, viscosity-pressure and density-pressure relations equations, and load balance equations simultaneously. The film thickness and pressure characteristics of the lubricant are discussed for various parameters.

II. THEORETICAL ANALYSIS

1. Average Type Reynolds Equations and Flow Factors

The constitutive relationship for a power-law fluid is as follows:

$$\tau_{ij} = mD^{n-1}\dot{\gamma}_{ij},\ D = \sqrt{2\dot{\gamma}_{ij}\dot{\gamma}_{ij}} \tag{1}$$

where m is viscosity consistency, τ_{ij} is the Cauchy stress deviator, $\dot{\gamma}_{ij}$ is the shear rate tensor, and n is the flow index. The conditions of $n > 1$, $n = 1$, and $n < 1$ correspond to a dilatant fluid, Newtonian fluid, and pseudoplastic fluid, respectively.

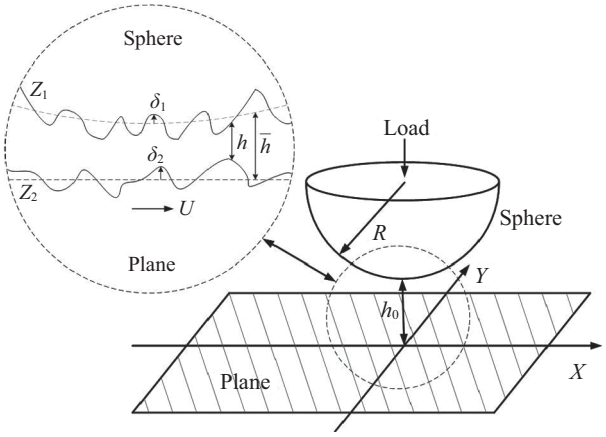

Fig. 1. Schematic of geometry of model problems.

As shown in Fig. 1, the contact geometry of two balls can be reduced to the contact geometry as an elastic ball and a rigid flat surface. For the steady state, isothermal, EHL circular contact problems with effects of surface roughness and flow rheology taken into account, the average type Reynolds equation [17] can be expressed in the following form as:

$$\frac{\partial}{\partial x}\left(\frac{h^{n+2}}{nm}\rho\phi_{xx}^{p}\frac{\partial p}{\partial x}\right)+\frac{\partial}{\partial y}\left(\frac{h^{n+2}}{m}\rho\phi_{yy}^{p}\frac{\partial p}{\partial y}\right)$$

$$=12u^{*n-1}\left[\bar{u}\frac{\partial\rho h}{\partial x}-u^{*}\frac{\sigma}{2}\frac{\partial\rho\phi_{xx}^{s}}{\partial x}\right] \tag{2}$$

where

$$\bar{u}=\frac{u_2+u_1}{2} \tag{3}$$

$$u^{*}=u_2-u_1 \tag{4}$$

The derived flow factors are:

$$\phi_{xx}^{p}=1+(n+2)\left(\frac{\sigma}{h}\right)^{2}\left[\frac{(n+1)}{2}-\frac{n+2}{\sqrt{n\gamma}+1}\right] \tag{5}$$

$$\phi_{yy}^{p}=1+(n+2)\left(\frac{\sigma}{h}\right)^{2}\left[\frac{(n+1)}{2}-\frac{(n+2)\sqrt{n\gamma}}{\sqrt{n\gamma}+1}\right] \tag{6}$$

$$\phi_{xx}^{s}=-(n+2)\left(\frac{\sigma}{h}\right)\left[\left(\frac{\sigma_2}{\sigma}\right)^{2}\frac{1}{\sqrt{n\gamma_2}+1}-\left(\frac{\sigma_1}{\sigma}\right)^{2}\frac{1}{\sqrt{n\gamma_1}+1}\right] \tag{7}$$

with

$$\frac{1}{\sqrt{n\gamma}+1}=\left(\frac{\sigma_2}{\sigma}\right)^{2}\frac{1}{\sqrt{n\gamma_2}+1}+\left(\frac{\sigma_1}{\sigma}\right)^{2}\frac{1}{\sqrt{n\gamma_1}+1} \tag{8}$$

$$\left(\frac{\sigma_2}{\sigma}\right)^2+\left(\frac{\sigma_1}{\sigma}\right)^2=1 \tag{9}$$

Eq. (2) can be expressed in the following dimensionless form as:

$$\frac{\partial}{\partial X}\left(\frac{H^{n+2}}{n\bar{m}}\bar{\rho}\phi_{xx}^{p}\frac{\partial P}{\partial X}\right)+\frac{\partial}{\partial Y}\left(\frac{H^{n+2}}{\bar{m}}\bar{\rho}\phi_{yy}^{p}\frac{\partial P}{\partial Y}\right)$$
$$=\lambda\left[u^{*n-1}\frac{\partial\bar{\rho}H}{\partial X}-\frac{u^{*n}\bar{\sigma}}{2\bar{u}}\frac{\partial\bar{\rho}\phi_{xx}^{s}}{\partial X}\right] \tag{10}$$

where

$$\lambda=\frac{12m_0b\bar{u}}{p_h}\left(\frac{R_x}{b^2}\right)^{n+1} \tag{11}$$

$\bar{m}$ and $\bar{\rho}$ are dependent on pressure. The boundary conditions for Eq. (10) are

$$P=0 \text{ at } X=X_{in};\ -1.8\le Y\le 1.8 \tag{12a}$$

$$P=0 \text{ at } Y=\pm 1.8;\ X_{in}\le X\le X_{end}=\varsigma(Y) \tag{12b}$$

$$P=\frac{dP}{dX}=0 \text{ at } X=\varsigma(Y) \text{ and } -1.8\le Y\le 1.8 \tag{12c}$$

2. Rheology Equation

Both the viscosity and density of the lubricant are assumed to be functions of pressure only, the relationship between viscosity and pressure used by Roelands [21] can be expressed as:

$$\bar{m}=\exp\left\{(9.67+\ln m_0)\left[-1+(1+5.1\times10^{-9}p)^{z'}\right]\right\} \tag{13}$$

where m_0 is the viscosity at the ambient pressure and z' is the pressure-viscosity index. According to Dowson and Higginson [11], the relationship between density and pressure is given as:

$$\bar{\rho}=\frac{\rho}{\rho_0}=1+\frac{0.6\times10^{-9}p}{1+1.7\times10^{-9}p} \tag{14}$$

3. Film Equation

Using the parabolic approximation for the geometry, the lubricant film thickness in the dimensionless form can be written as:

$$H(X,Y)=H_{00}+\frac{X^2+Y^2}{2}$$
$$+\frac{2}{\pi^2}\int_{-\infty}^{\infty}\int_{-\infty}^{\infty}\frac{P(X',Y')dX'dY'}{\left[\left(X-X'\right)^2+\left(Y-Y'\right)^2\right]^{1/2}} \tag{15}$$

Table 1. Computational data.

Properties of lubricants	
G (Material parameter)	3500
Inlet viscosity of lubricant, Pa-s	0.04
Inlet density of lubricant, kg/m^3	846
Pressure viscosity coefficient, 1/GPa	15.91
Pressure-viscosity index (Roelands)	0.4836
Properties of balls	
Reduced radius, m	0.02
Density of balls, kg/m^3	7850
Elastic modulus of balls, GPa	200
Poisson's ratio of balls	0.3

where H_{00} is a constant. Discretizing the elastic deformation integral, the film shape is given as:

$$H_{i,j}=H_{00}+\frac{(X_{i,j}^2+Y_{i,j}^2)}{2}+\frac{2}{\pi^2}\sum_{k=1}^{n_x}\sum_{l=1}^{n_y}K_{ikjl}P_{kl}\,. \tag{16}$$

where the coefficients are determined analytically assuming the uniform pressure over the various rectangular areas in the contact area, the influence coefficients, K_{ikjl}, are computed according to Lubrecht [18]. The assumptions of roughness deformation are: large wavelength components deform almost completely whereas small wavelength components pass through the conjunction almost undeformed [26].

4. Force Balance Equation

The applied normal load on the balls must be supported by the generated hydrodynamic pressure in the contact region and is assumed to be a constant as:

$$\int_{-\infty}^{\infty}\int_{-\infty}^{\infty}P(X,Y)dXdY=\frac{2\pi}{3} \tag{17}$$

III. RESULTS AND DISCUSSION

In Table 1, the material properties of lubricants and balls for the present analysis are listed. The solutions of the film thickness and the pressure distributions of the isothermal EHL point-contact problems are obtained by solving the average Reynolds type equation, the load balance equation, the viscosity-pressure and density-pressure relations equations, and the elastic deformation equation simultaneously. The multilevel multi-integration (MLMI) algorithm [4] and the Gauss-Seidel iterative method are utilized to solve the pressure and film thickness distributions of the EHL problem with effects of surface roughness and flow rheology. Most cases presented in this paper use a domain extending from X_{in} = –4.0 to X_o = 1.4, and $-1.8\le Y\le 1.8$. The dimensionless outlet location, $X_{end}=\varsigma(Y)$, is determined by the complementary theory of mathematical programming. Typical problem with

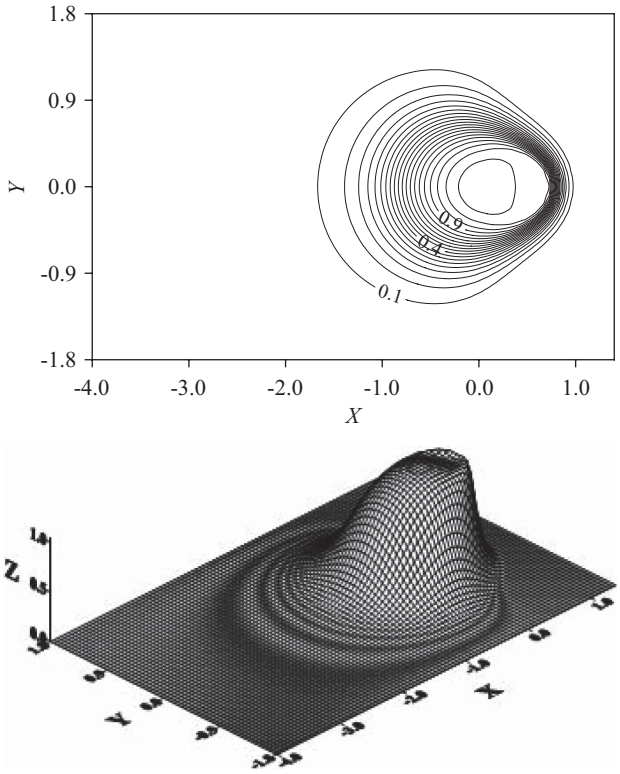

Fig. 2. Contour map of pressure and 3-D plot of pressure.

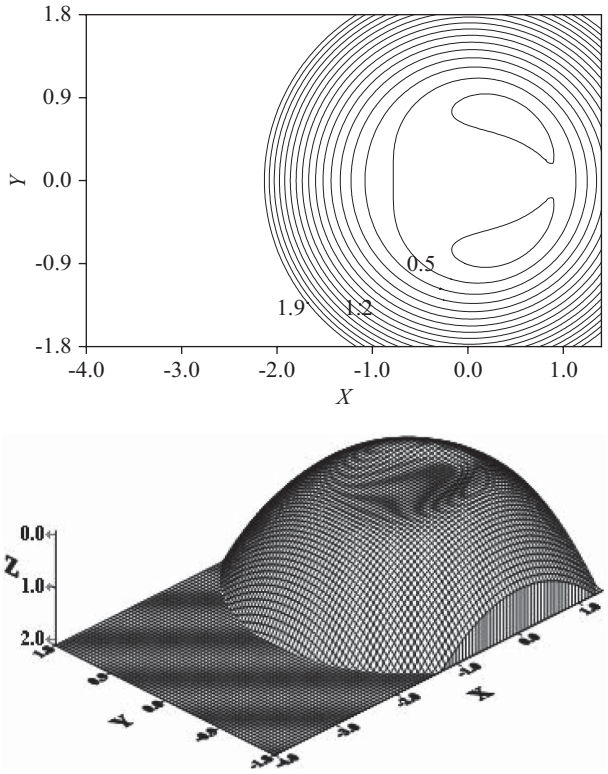

Fig. 3. Contour map of film thickness and 3-D plot of film thickness.

$W = 1.932 \times 10^{-7}$, $U = 1.364 \times 10^{-11}$, $G = 3500$, $\gamma_1 = \gamma_2 = \gamma = 0.1$, $\bar{\sigma} = 0.081$, $\bar{\sigma}_1 = \bar{\sigma}_2 = 0.057$, $n = 0.98$, and S = -2.0 is solved. A grid size of 33×97 grids in the half domain (symmetry *w.r.t.* X-axis) is used for the evaluation of pressure and elastic deformation.

In Figs. 2 and 3, the pressure distributions and film thickness are plotted, respectively. It is interesting to find a pressure spike occurs in Fig. 2. The associated film shape and film thickness contour plot shown in Fig. 3 shows that the film thickness contour plot in the pressure spike region can be detected as the U-shaped region of high gradients of the film thickness. This behavior can be explained by the average type Reynolds equation where the large second derivatives of the pressure spike should be compensated by large gradients in the film thickness. The pressure spike and U-shaped region are the main characteristic of EHL.

As shown in Figs. 4(a) and 4(b), the effects of Peklenik number on the pressure distributions and film thickness are plotted in *x*-direction and *y*-direction, respectively. The longitudinal type roughness ($\gamma = 10$) and transverse type roughness ($\gamma = 1/10$) are discussed. The Peklenik number is defined as the ratio of the half-correlation lengths of the representative asperity in the principal directions. The transverse direction is orthogonal to the sliding direction. The transverse type roughness resists the flow in sliding direction (*x*-dir.), and enhances the flow in the perpendicular direction (*y*-dir.). Due to the present fixed load conditions, the pressure distributions of these two types should have the same load capacities by integrating the pressure distributions over the pressure acting area. Fig. 4(a) shows that the transverse type roughness has a small increase in pressure and film thickness near the high pressure region as compare to those of the longitudenal type roughness. On the contrary, we have a small decrease in pressure and film thickness in the inlet region for transverse type roughness as compared to that for longitudinal type roughness. Near the smallest film thickness region, the effect of surface roughness becomes important. Therefore, we have significant pressure difference between transversely and longitudinal type roughness as compared to those in inlet region. The symmetric nature of film thickness and pressure distribution with respect to the axis $X = 0$, are plotted as shown in Fig. 4(b). Under the conditions of fixed load, we have the larger pressure and film thickness near the central region for transverse type roughness, and the smaller pressure and film thickness outside the central region as compared to the pressure distribution of longitudinal type roughness.

To discuss the effects of standard deviation of composite surfaces ($\sigma = \sqrt{\sigma_1^2 + \sigma_2^2}$) on the film thickness and pressure distribution, the *X*-cross section and *Y*-cross section plots are plotted as shown in Figs. 5(a) and 5(b), respectively. Larger standard derivations result in larger pressure distribution and film thickness near the central region. The reverse effects of pressure and film thickness outside the central region come from the fixed load condition requirement.

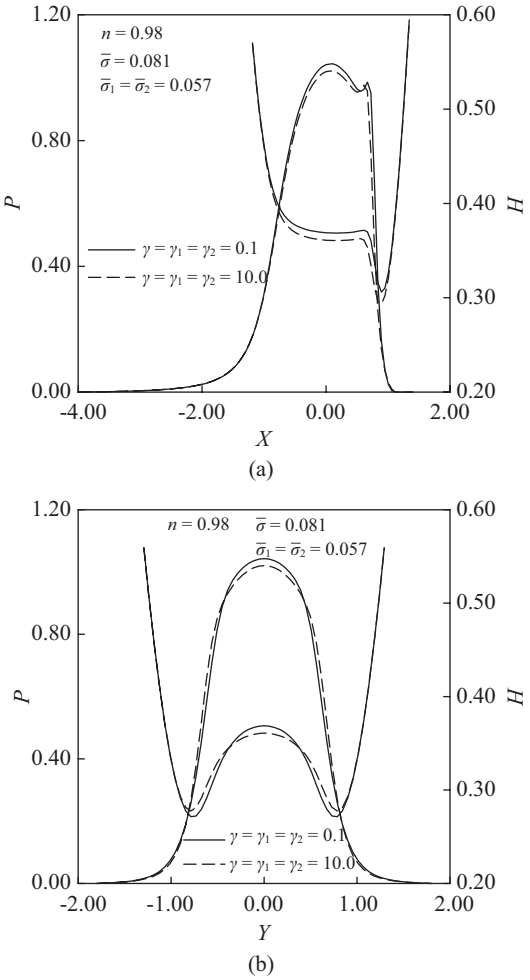

Fig. 4. (a) *X*-cross section plot, and (b) *Y*-cross section plot of pressure and film shapes obtained using two Peklenik numbers.

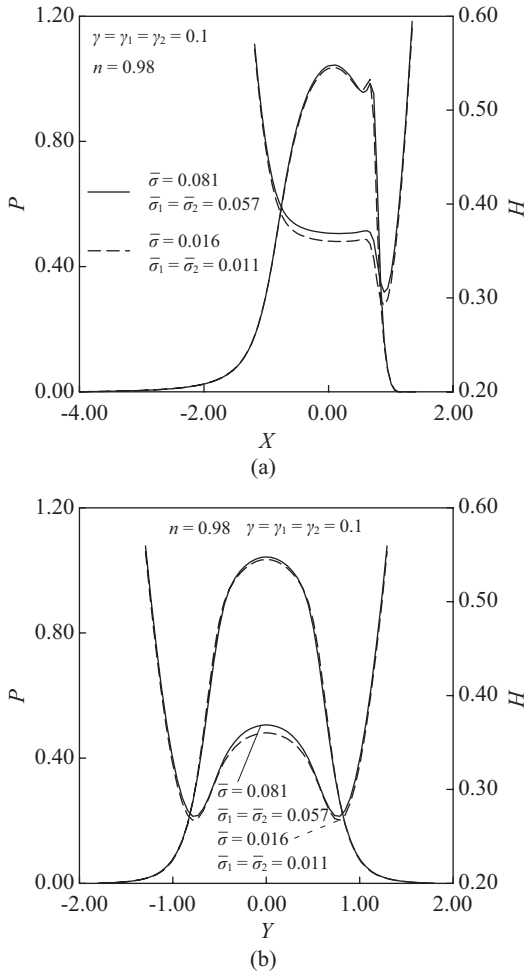

Fig. 5. (a) *X*-cross section plot, and (b) *Y*-cross section plot of pressure and film shapes obtained using two standard derivations of composite roughness.

Moreover, the effects of power-law flow index (n) on the pressure and film thickness are shown in Figs. 6(a) ($Y = 0$) and 6(b) ($X = 0$). Near the central region, the pressure distributions follow the ($n = 1.02$) > ($n = 1.00$) > ($n = 0.98$). However, the reverse properties for pressure occur in outlet region come from the fixed load condition requirement. Fig. 6(b) ($X = 0$) show the effects of power-law flow index (n) on the pressure and film thickness in y-direction. Near the central region, the pressure distributions follow the ($n = 1.02$) > ($n = 1.00$) > ($n = 0.98$). However, the reverse properties for pressure occur outside the central region inside the Hertzian contact, and the larger the flow index, the larger the pressure in outlet region. The film thickness follow the ($n = 1.02$) > ($n = 1.00$) > ($n = 0.98$) in all regions. The larger flow index results in larger effective viscosity and thus larger pressure and film thickness near the central region. In addition, the larger pressure spike occurs as the flow index increases.

As shown in Fig. 7, the central pressure (P_c), and central film thickness (H_c) are plotted as functions of Peklenik number (γ) for flow index $n = 0.98$, 1.00, and 1.02. The central pressure (P_c), and central film thickness (H_c) decrease as γ increases. The flow in X-direction is more restricted by the transverse type roughness as compared to that by longitudinal type roughness. Therefore, we have higher central pressure (P_c), and central film thickness (H_c) as the Peklenik number (γ) decreases. As shown in Fig. 8, the central pressure (P_c), and central film thickness (H_c) are plotted as functions of the composite standard deviation ($\bar{\sigma}$) of roughness for flow index $n = 0.98$, 1.00, and 1.02. The central pressure (P_c), and central film thickness (H_c) increase as $\bar{\sigma}$ increases. As shown in Fig. 9, the central pressure (P_c), and central film thickness (H_c) are plotted as functions of flow index n. The P_c and H_c increase as the flow index increases.

IV. CONCLUSIONS

The effects of surface roughness on the film thickness and pressure are studied numerically based on power law fluid model under point contact EHL conditions. In EHL problems,

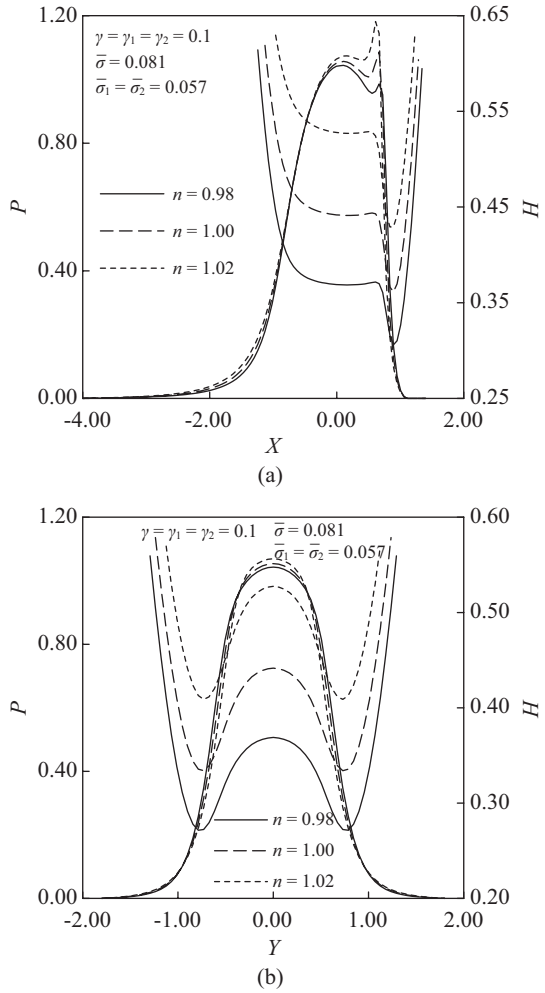

Fig. 6. (a) *X*-cross section plot, and (b) *Y*-cross section plot of pressure and film shapes obtained using three power law indices of lubricant.

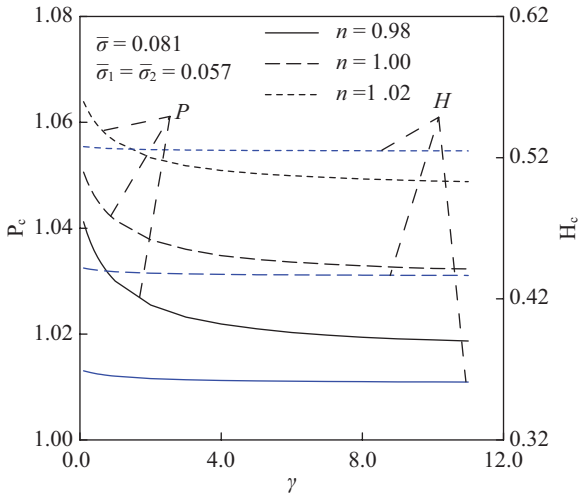

Fig. 7. Central pressure and film thickness plotted as functions of Peklenik numbers.

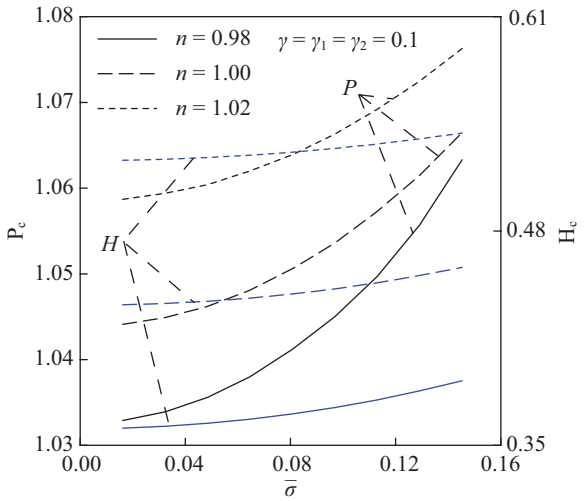

Fig. 8. Central pressure and film thickness plotted as functions of composite standard variation.

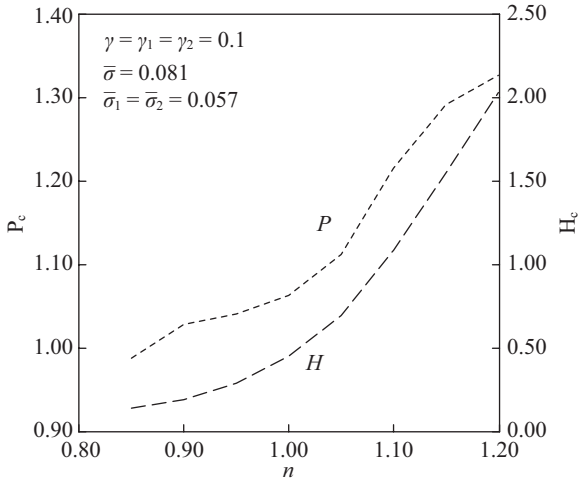

Fig. 9. Central pressure and film thickness plotted as functions of flow index.

the film thickness is usually comparable to the height of surface roughness in the contact zone. Therefore, the effect of surface roughness becomes important. The results show that the effects of Peklenik number are significant near the central contact region, and the transverse type roughness enhances the pressure and film thickness. Moreover, the effects of composite roughness derivation are also significant near the central contact region, and higher composite roughness derivation enhances the pressure and film thickness. As compared to the above two effects, the flow index is the most significant parameter that affect the calculated pressure and film thickness. The central pressure and central film thickness increase as the flow index increases.

ACKNOWLEDGMENTS

The authors would like to express their appreciation to the National Science Council (NSC 99-2221-E-214-011) in Taiwan for financial support.

NOMENCLATURE

b	semiwidth of hertzian contact (m), $(3wR_x/2E')^{1/3}$
E'	equivalent Young's modulus (Pa)
G	dimensionless material parameter, $\alpha E'$
h	film thickness (m)
H	dimensionless film thickness, hR_x/b^2
Hc	dimensionless central film thickness
H_{00}	dimensionless constant defined in Eq. (15)
m	viscosity consistency ($Pa - s^n$)
m_0	reference viscosity consistency ($Pa - s^n$)
$\bar{m}$	dimensionless viscosity, m/m_0
n	flow index
p	pressure (Pa)
p_h	maximum Hertzian pressure (Pa)
P	dimensionless pressure, p/p_h
R_x	reduced radius of curvature in x-direction (m)
S	slip/roll ratio, $(u_2 - u_1)/\bar{u}$
$\bar{u}$	average velocity (m/s), $(u_2 + u_1)/2$
u^*	$u_2 - u_1$ (m/s)
U	dimensionless speed parameter, $m_0\bar{u}/E'R_x$
w	load (N)
W	dimensionless load, $W = w/E'R_x^2$
x, y, z	coordinates (m)
X, Y, Z	dimensionless coordinate, $X = x/b$, $Y = y/b$, $Z = z/h$
z'	Roelands' pressure-viscosity index
α	pressure-viscosity coefficient (Pa^{-1})
σ	standard deviation of composite roughness (m)
$\bar{\sigma}$	dimensionless standard deviation of composite roughness, $\sigma R_x/b^2$
ρ	density of lubricant (kg/m^3)
ρ_0	density of lubricant at ambient pressure (kg/m^3)
$\bar{\rho}$	dimensionless density of lubricant, ρ/ρ_0
γ	Peklenik parameter

REFERENCE

1. Bair, S. and Winer, W. O., "A rheological model for elastohydrodynamic contacts based in primary laboratory data," *ASME Journal of Lubrication Technology*, Vol. 101, No. 3, pp. 258-265 (1979).
2. Bell, I. F., *Elasto-Hydrodynamic Effects in Lubrication*, MSc Thesis, University of Manchester (1961).
3. Bhattacharjee, R. C. and Das, N. C., "Power law fluid model incorporated into elastohydrodynamic lubrication theory of line contact," *Tribology International*, Vol. 29, No. 5, pp. 405-413 (1996).
4. Brandt, A. and Lubrecht, A. A., "Multilevel matrix multiplication and fast solution of integral equations," *Journal of Computational Physics*, Vol. 90, pp. 348-370 (1990).
5. Chang, L. and Webster, M. N., "A study of elastohydrodynamic lubrication of rough surfaces," *Transaction of the ASME Journal of Tribology*, Vol. 113, pp. 110-113 (1991).
6. Cheng, H. S. and Dyson, A., "Elastohydrodynamic lubrication of circumferentially ground rough disks," *ASLE Transactions*, Vol. 21, No. 1, pp. 25-40 (1978).
7. Christensen, H., "Stochastic models for hydrodynamic lubrication of rough surfaces," *Proceedings of the Institution of Mechanical Engineers*, Vol. 184, No. 1, pp. 1013-1026 (1969/70).
8. Chu, H. M., Li, W. L., and Chang, Y. P., "Thin film elastohydrodynamic lubrication - a power-law fluid model," *Tribology International*, Vol. 39, pp. 1474-1481 (2006).
9. Chu, H. M., Li, W. L., Chang, Y. P., and Huang, H. C., "Effects of Couple Stress on Elastohydrodynamic Lubrication at Impact Loading," *ASME Journal of Tribology*, Vol. 130, No. 1, pp. 011010-1-011010-8 (2008).
10. Dien, I. K. and Elrod, B. C., "A generalized steady state Reynolds equation for non-Newtonian fluids, with application to journal bearings," *ASME Journal of Lubrication Technology*, Vol. 105, No. 3, pp. 385-390 (1983).
11. Dowson, D. and Higginson, G. R., *Elastohydrodynamic Lubrication*, Pergamon Press, pp. 88-92 (1966).
12. Eringen, A. C., "Thoery of micropolar fluids," *Journal of Mathematics and Mechanics*, Vol. 16, pp. 1-18 (1966).
13. Greenwood, J. A. and Tripp, J. H., "The contact of two nominally flat rough surfaces," *Proceedings of the Institution of Mechanical Engineers*, Vol. 185, No. 1, pp. 625-633 (1970/71).
14. Hu, Y. Z. and Zhu, D., "A full numerical solution to the mixed lubrication in point contacts," *Transaction of the ASME Journal of Tribology*, Vol. 122, pp. 1-9 (2000).
15. Ivonen, H. T. and Hamrock, B. J., "A non-Newtonian fluid model for elastohydrody- namic lubrication of rectangular contacts," *Proceedings of the Fifth International Congress on Tribology*, Helsinki, Finland, pp. 178-183 (1989).
16. Lee, R. T. and Hamrock, B. J., "A circular non-Newtonian fluid model: part I - used in elastohydrodynamic lubrication," *ASME Journal of Tribology*, Vol. 112, pp. 486-496 (1990).
17. Li, W. L., Weng, C. I., and Lue, J. I., "Surface roughness effects in journal bearing with non-newtonian lubricants," *STLE, Tribology Transaction*, Vol. 39, No. 4, pp. 819-826 (1996).
18. Lubrecht, A. A., *The Numerical Solution of the Elastohydrodynamically Lubricated Line and Point Contact Problem, Using Multigrid Techniques*, Ph.D. Thesis, University of Twente Enschede (ISBN 90-9001583-3) (1987).
19. Patir, N. and Cheng, H. S., "An average flow model for determining effects of three-dimensional roughness on partial hydrodynamic lubrication," *ASME Journal of Lubrication Technology*, Vol. 100, No, 1, pp. 12-17 (1978).
20. Prakash, J. and Sinha, P., "Lubrication theory for micropolar fluids and its application to a journal bearing," *International Journal of Engineering Science*, Vol. 13, pp. 217-232 (1975).
21. Roelands, C. J. A., Vlugter, J. C., and Watermann, H. I., "The viscosity temperature pressure relationship of lubricating oils and its correlation with chemical constitution," *ASME Journal of Basic Engineering*, Vol. 85, pp. 601-606 (1963).
22. Sadeghi, F. and Sui, P. C., "Compressible elastohydrodynamic lubrication of rough surfaces," *Transaction of the ASME Journal of Tribology*, Vol. 111, No. 1, pp. 56-62 (1989).
23. Sinha, P. and Singh, C., "Non-Newtonian squeeze films in spherical bearings," *Wear*, Vol. 68, pp. 133-140 (1981).
24. Stokes, V. K., "Couple stresses in fluids," *Physics of Fluids*, Vol. 9, pp. 1709-1715 (1966).
25. Tanner, R. I., "Flow of viscoelastic non-Newonian lubricants," *ASLE Transactions*, Vol. 8, pp. 179-183 (1965).
26. Venner, C. H. and Lubrecht, A. A., "An engineering tool for the quantitative prediction of general roughness deformation in EHL contacts based on harmonic waviness attenuation," *Proceedings of the Institution of Mechanical Engineers, Part J: Journal of Engineering Tribology*, Vol. 219, pp. 303-312 (2005).
27. Xu, G. and Sadeghi, F., "Thermal EHL analysis of circular contacts with measured surface roughness," *Transaction of the ASME Journal of Tribology*, Vol. 118, pp. 473-482 (1996).
28. Zuh, D and Cheng, H. S., "Effect of surface roughness on the point contact EHL," *Transaction of the ASME Journal of Tribology*, Vol. 110, No. 1, pp. 32-37 (1988).